

OSCILLATING TAYLOR-COUETTE: SYMMETRY BREAKING AND IMPERFECTIONS

F. Marques¹ V. Iranzo¹ J. M. Lopez²

¹Univeristad Politècnica de Catalunya; 08034 Barcelona, Spain; marques@fa.upc.es, iranzo@fa.upc.es

²Arizona State University; Tempe, AZ 85287-1804, USA; lopez@math.la.asu.edu

Abstract

Finite Taylor-Couette flow with axial harmonic oscillation of the inner cylinder is simulated. Three-tori solutions exist and undergo homoclinic and heteroclinic bifurcations, including a new gluing bifurcation. A discrete space-time glide-reflection symmetry influences the dynamics. The effect of imperfections in the harmonic oscillation is elucidated.

The results presented here are of 3-tori solutions from a fully resolved numerical computation of the Navier-Stokes equations with no-slip boundary conditions, restricted to an axisymmetric subspace, and as such, the obtained 3-tori solutions are solutions to the full Navier-Stokes equations. The system in question is the flow between two co-axial cylinders of finite extent with stationary top and bottom endwalls. The outer cylinder is also stationary while the inner cylinder rotates at constant angular velocity Ω_i and oscillates in the axial direction with velocity $W \sin \Omega_f t$. Its radius is r_i , the radius of the outer stationary cylinder is r_o , and their length is L ; the annular gap between the cylinders is $d = r_o - r_i$. These parameters are combined to give the following nondimensional governing parameters: the radius ratio $e = r_i/r_o$, the length to gap ratio $\Lambda = L/d$, the Couette flow Reynolds number $Ri = dr_i \Omega_i / \nu$, the axial Reynolds number $Ra = dW/\nu$, and the nondimensional forcing frequency $\omega_f = d^2 \Omega_f / \nu$, where ν is the kinematic viscosity of the fluid. The basic flow is time-periodic with period $T_f = 2\pi/\omega_f$ and synchronous with the forcing, and it is independent of the azimuthal coordinate.

The incompressible Navier-Stokes equations governing this problem are invariant to two symmetry groups. One corresponds to rotations around the common axis of the cylinders, $SO(2)$. The other, Z_2 , is generated by the discrete symmetry S , involving time and the axial coordinate; it is a reflection about the mid-plane orthogonal to the axis with a simultaneous time-translation of a half forcing period, satisfying $S^2 = I$. In this study we solve the system in an axisymmetric subspace invariant to $SO(2)$.

The axisymmetric Navier-Stokes equations have

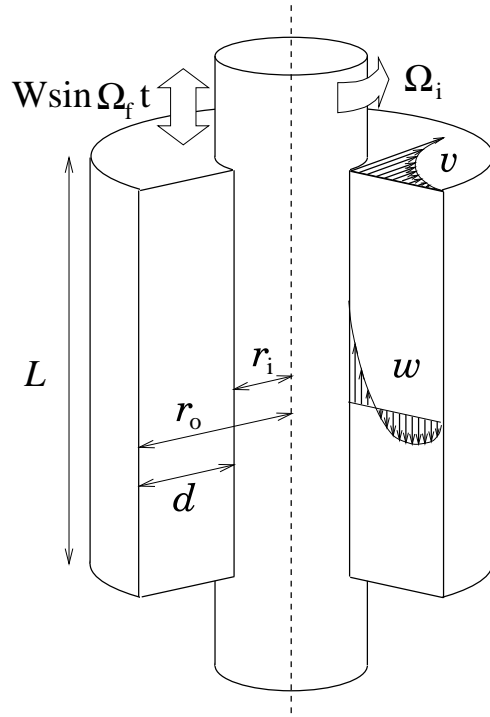


Figure 1: Schematic of the flow configuration.

been solved with the spectral scheme described in Lopez *et al.* (2000), using 80 axial and 64 radial modes, and a time-step $\delta t = T_f/200$. We have studied a one-dimensional route in parameter space, considering variations in Ri , and keeping all other parameters fixed ($\Lambda = 10$, $e = 0.905$, $Ra = 80$, $\omega_f = 30$). As Ri is increased, the system undergoes a sequence of local and global bifurcations and becomes chaotic. The route to chaos obtained involves a new and convoluted symmetry breaking, involving heteroclinic, homoclinic, and gluing bifurcations of \mathbb{T}^3 .

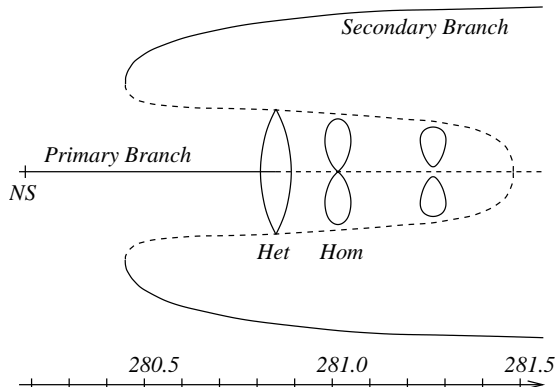


Figure 2: Bifurcation diagram showing the primary, secondary and \mathbb{T}^3 branches; the dashed lines are the unstable branches.

An overall description of our one-dimensional path is schematically presented in Fig. 2. The solid curves correspond to stable \mathbb{T}^1 , \mathbb{T}^2 , and \mathbb{T}^3 solution branches which were encountered. The dashed curves connecting them are conjectured, based on properties of the stable solutions. The primary branch, consisting of S -invariant \mathbb{T}^1 , undergoes a supercritical Naimark-Sacker bifurcation to an S -invariant \mathbb{T}^2 . This is the generic scenario of a Z_2 -symmetric Naimark-Sacker (Kuznetsov, 1998). The resulting \mathbb{T}^2 is S -invariant, but obviously the solutions (trajectories) on it are not S -invariant by virtue that the two frequencies on the \mathbb{T}^2 are incommensurate. This \mathbb{T}^2 loses stability, but remains S -invariant as Ri is increased, and solution trajectories evolve to a \mathbb{T}^3 .

We have located a range ($Ri \in [280.89, 281.26]$) where stable 3-tori solutions exist. The identification of such solutions has been significantly helped due to the imposed periodic forcing, which implies the existence of a global Poincaré map, \mathbf{P} , for the system (i.e. strobing at the forcing frequency ω_f). The power spectral density (PSD) of the time series of Γ , the vertical angular momentum at a convenient point in the annulus, has a main peak at the forcing frequency, $\omega_f = 30$, a second frequency at $\omega_s \approx 5.2$,

and their linear combinations since these are incommensurate. The frequency ω_s has been found to be associated with the coupling between the endwall vortices and the sidewall jets Lopez *et al.* (2000). The PSD also possesses a very low frequency ω_{VLF} which is three orders of magnitude smaller than ω_s . Due to the large spectral gaps between these three incommensurate frequencies we have been able to unambiguously characterize these solutions as 3-tori.

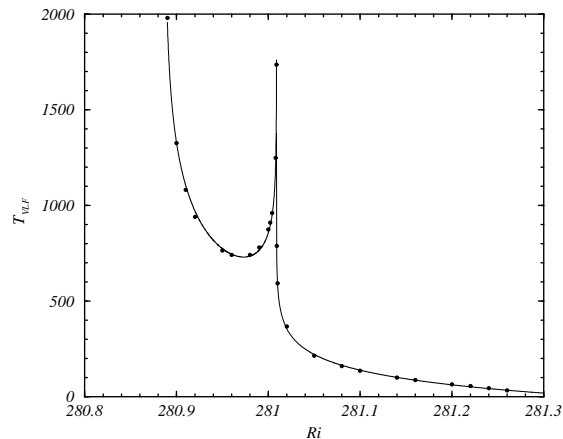


Figure 3: Variation of $T_{VLF} = 2\pi/\omega_{VLF}$ with Ri . Symbols are computed values, and solid lines are log fits.

Over the range of Ri where 3-tori solutions exist, $T_{VLF} = 2\pi/\omega_{VLF}$ experiences dramatic changes, as shown in Fig. 3. T_{VLF} fits very well the logarithmic form $T_{VLF} \sim c \ln(1/|Ri - Ri_{crit}|) + d$, strongly suggesting that the homoclinic/heteroclinic behavior dominates the dynamics over the whole interval.

The range of Ri where 3-tori exist consists of two branches; for $280.89 = Ri_{het} < Ri < Ri_{hom} = 281.01$, there is a single S -symmetric 3-torus and for $Ri > Ri_{hom}$ a pair of non-symmetric, but symmetrically related, 3-tori. The first branch starts in a heteroclinic bifurcation schematically shown in Fig. 4, and is related to the second branch via a homoclinic bifurcation at $Ri = Ri_{hom}$. In this homoclinic bifurcation an S -symmetric 3-torus splits in two S -related 3-tori. Analogous gluing bifurcations of limit cycles in systems with Z_2 symmetry have been analyzed in Glendinning (1984), and in Armbruster *et al.* (1996) for systems with more complex (D_4) symmetries. We have found for the first time a gluing bifurcation of 3-tori in a real fluid system.

Continuing the \mathbb{T}^3 branch to lower Ri , the branch ceases to exist at a heteroclinic bifurcation as it collides with two S -symmetrically related unstable \mathbb{T}^2 ; the \mathbb{T}^3 is S -invariant. Increasing Ri , the \mathbb{T}^3 becomes homoclinic to an S -invariant unstable \mathbb{T}^2 , which we conjecture is the unstable \mathbb{T}^2 from the pri-

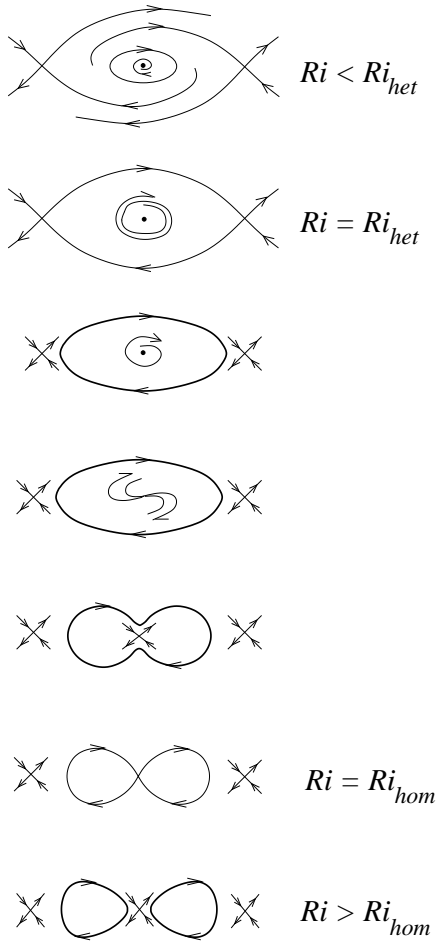


Figure 4: Schematic of the bifurcation sequence for the 3-tori solutions. In this schematic, 2-tori are represented as fixed points and 3-tori as cycles.

mary branch. The conjecture is based on the close similarities of the corresponding oscillatory flows on the stable \mathbb{T}^2 and the unstable \mathbb{T}^2 to which the \mathbb{T}^3 becomes homoclinic to. The secondary frequency, ω_s , is continuous between the two \mathbb{T}^2 , further supporting this conjecture. At the homoclinic point, the \mathbb{T}^3 suffers a symmetry breaking gluing bifurcation. This is the only symmetry breaking bifurcation we have observed in this system. The importance of the Z_2 symmetry in the Taylor-Couette problem, and its association with complex dynamics (e.g. homoclinic and Shil'nikov bifurcations) was pointed out by Mullin & Cliffe (1986), and was also reviewed in Mullin (1993).

Increasing Ri beyond a critical value, the \mathbb{T}^3 branch can not be continued further and the flow evolves onto a \mathbb{T}^2 that is not S -invariant. In fact, there are two such \mathbb{T}^2 branches, symmetrically related, along which a standard (i.e. not influenced by symmetries) route to chaos via quasi-periodicity and locking in

resonance horns, and torus break-up is observed.

The three \mathbb{T}^2 to which the \mathbb{T}^3 are either heteroclinically or homoclinically asymptotic to are the organizing centers of the dynamics of the \mathbb{T}^3 . In fact, the \mathbb{T}^3 flows are essentially slow drifts, with very low frequency (VLF), between the unstable \mathbb{T}^2 . Similar very low frequency states have also been observed experimentally (von Stamm *et al.*, 1994, 1996; Busse *et al.*, 1998) in an unforced Taylor-Couette flow with aspect ratio of order 10, as is the aspect ratio in our computations. Since their system was unforced, the VLF states manifested themselves as \mathbb{T}^2 . Furthermore, those observed VLF states are reported to be axisymmetric modes of oscillation between the endwalls, even though the underlying flow is non-axisymmetric (von Stamm *et al.*, 1996). We can reasonably expect that our axisymmetric \mathbb{T}^3 solutions, even if they are unstable to non-axisymmetric disturbances, continue to play an important role in the flow dynamics.

How are the various observed stable and unstable \mathbb{T}^2 connected? As Ri decreases along the secondary branch, ω_s increases from 3.2 to 3.9, getting close to ω_s values on the primary \mathbb{T}^2 and the \mathbb{T}^3 branches. This leads us to conjecture that the unstable \mathbb{T}^2 heteroclinic to the \mathbb{T}^3 and the stable secondary \mathbb{T}^2 branch merge at a saddle-node bifurcation of \mathbb{T}^2 and cease to exist at lower Ri . This is the lowest co-dimension bifurcation consistent with the observed characteristics of the respective \mathbb{T}^2 . All possible bifurcations of \mathbb{T}^2 is a subject that has not yet been exhaustively studied, but Chenciner & Iooss (1979) describe the most likely scenarios associated with a real eigenvalue crossing the unit circle through ± 1 or the crossing of a pair of complex conjugate eigenvalues. Both the -1 and the complex conjugate crossing would introduce a new frequency, which is not the case in our system; the $+1$ crossing, since there is no symmetry involved, corresponds to a saddle-node.

We also conjecture that on increasing Ri , the unstable \mathbb{T}^2 associated with the \mathbb{T}^3 branch merge in a pitchfork bifurcation of \mathbb{T}^2 . We have been able to observe the flows on (near) these three \mathbb{T}^2 and they are all very similar, so it is reasonable that at large enough Ri , they merge. The simplest bifurcation consistent with one symmetric and two symmetrically related \mathbb{T}^2 is the pitchfork. These results have been reported in Lopez & Marques (2000); Marques *et al.* (2001).

Imperfections are always present in any real experiment, and it is important to know how the reported bifurcation diagram changes in the presence of small perturbations that breaks the space-time glide-reflection symmetry S . In particular, do the \mathbb{T}^3 solutions remain under perturbations? And how

is the bifurcation diagram in Fig. 2 modified by the presence of imperfections?

We have considered only one kind of imperfection, related to the harmonic character of the oscillation of the inner cylinder. It is very difficult to obtain a pure harmonic oscillation in the lab, and with any deviation of harmonicity, S ceases to be a symmetry of the system. We have considered non-harmonic axial oscillations of the form $W(\sin \Omega_f t + \epsilon \sin 2\Omega_f t)$, where the parameter ϵ is a measure of the imperfection. Preliminary results suggest that the two secondary branches are no longer symmetric, and the three-tori branch exists for a larger Ri parameter range. Moreover, the heteroclinic and gluing bifurcations become standard homoclinic bifurcations of \mathbb{T}^3 colliding with an unstable \mathbb{T}^2 , as fig. 5 shows.

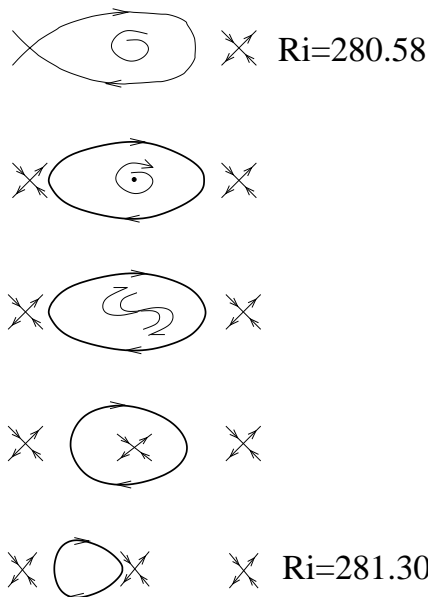


Figure 5: Schematic of the 3-tori bifurcation sequence for $\epsilon \neq 0$. In this schematic, 2-tori are represented as fixed points and 3-tori as cycles.

We also expect that the pitchfork bifurcation of unstable \mathbb{T}^2 unfolds into saddle-node bifurcations, as shown schematically in fig. 6.

Acknowledgement

This work was supported by NSF grants INT-9732637 and CTS-9908599 (USA), and DGICYT grant PB97-0685 (Spain)

References

ARMBRUSTER, D., NICOLAENKO, B., SMAOUI, N. & CHOSSAT, P. 1996 Symmetries and dynamics for 2-d navier-stokes flow. *Physica D* **95**, 81–93.

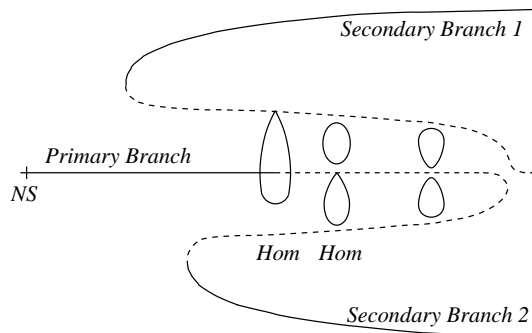


Figure 6: Bifurcation diagram showing the primary, secondary and \mathbb{T}^3 branches for $\epsilon \neq 0$; the dashed lines are the unstable branches.

BUSSE, F. H., PFISTER, G. & SCHWABE, D. 1998 Formation of dynamical structures in axisymmetric fluid systems. In *Evolution of Spontaneous Structures in Dissipative Continuous Systems* (ed. F. H. Busse & S. C. Müller), *Lecture Notes in Physics*, vol. m55, pp. 86–126. Springer.

CHENCINER, A. & IOOSS, G. 1979 Bifurcations de tores invariants. *Arch. Ration. Mech. An.* **69** (2), 109–198.

GLENDINNING, P. 1984 Bifurcations near homoclinic orbits with symmetry. *Phys. Lett.* **103A**, 163–166.

KUZNETSOV, Y. A. 1998 *Elements of Applied Bifurcation Theory, Second Edition*. Springer-Verlag.

LOPEZ, J. M. & MARQUES, F. 2000 Dynamics of 3-tori in a periodically forced Navier-Stokes flow. *Phys. Rev. Lett.* **85**, 972–975.

LOPEZ, J. M., MARQUES, F. & SHEN, J. 2000 Endwall effects in a periodically forced centrifugally unstable flow. *Fluid Dynam. Res.* **27**, 91–108.

MARQUES, F., LOPEZ, J. M. & SHEN, J. 2001 A periodically forced flow displaying symmetry breaking via a three-tori gluing bifurcation and two-tori resonances. *Physica D* **156**, 81–97.

MULLIN, T. 1993 Disordered fluid motion in a small closed system. *Physica D* **62**, 192–201.

MULLIN, T. & CLIFFE, K. A. 1986 Symmetry breaking and the onset of time dependence in fluid mechanical systems. In *Nonlinear Phenomena and Chaos* (ed. S. Sarkar), pp. 96–112. Adam Hilger.

VON STAMM, J., BUZUG, T. & PFISTER, G. 1994 Frequency locking in axisymmetric Taylor-Couette flow. *Phys. Lett. A* **194**, 173–178.

VON STAMM, J., GERDTS, U., BUZUG, T. & PFISTER, G. 1996 Symmetry breaking and period doubling on a torus in the VLF regime in Taylor-Couette flow. *Phys. Rev. E* **54** (5), 4938–4957.